

Modeling of dielectric and piezoelectric response of 1-3 type piezocomposites

R. Jayendiran and A. Arockiarajan

Citation: *Journal of Applied Physics* **112**, 044107 (2012); doi: 10.1063/1.4748057

View online: <http://dx.doi.org/10.1063/1.4748057>

View Table of Contents: <http://scitation.aip.org/content/aip/journal/jap/112/4?ver=pdfcov>

Published by the [AIP Publishing](#)

Articles you may be interested in

Complete set of elastic, dielectric, and piezoelectric constants of [011]C poled rhombohedral $\text{Pb}(\text{In}_{0.5}\text{Nb}_{0.5})\text{O}_3\text{-Pb}(\text{Mg}_{1/3}\text{Nb}_{2/3})\text{O}_3\text{-PbTiO}_3\text{:Mn}$ single crystals

J. Appl. Phys. **113**, 074106 (2013); 10.1063/1.4792661

Large and temperature-independent piezoelectric response in $\text{Pb}(\text{Mg}_{1/3}\text{Nb}_{2/3})\text{O}_3\text{-BaTiO}_3\text{-PbTiO}_3$

Appl. Phys. Lett. **101**, 192901 (2012); 10.1063/1.4765347

Study of effective properties of modified 1-3 piezocomposites

J. Appl. Phys. **104**, 064120 (2008); 10.1063/1.2975343

Piezoelectric properties and hardening behavior of $\text{K}_{0.5}\text{Cu}_{1.3}\text{Ta}_{10}\text{O}_{29}$ -doped $\text{K}_{0.5}\text{Na}_{0.5}\text{NbO}_3$ ceramics

J. Appl. Phys. **103**, 064105 (2008); 10.1063/1.2896588

Dielectric and piezoelectric properties of 001 fiber-textured $0.675 \text{Pb}(\text{Mg}_{1/3}\text{Nb}_{2/3})\text{O}_3\text{-}0.325 \text{PbTiO}_3$ ceramics

J. Appl. Phys. **93**, 4072 (2003); 10.1063/1.1554488



Not all AFMs are created equal
Asylum Research Cypher™ AFMs
There's no other AFM like Cypher

www.AsylumResearch.com/NoOtherAFMLikeIt

OXFORD
INSTRUMENTS
The Business of Science®

Modeling of dielectric and piezoelectric response of 1-3 type piezocomposites

R. Jayendiran^{a)} and A. Arockiarajan^{b)}

Department of Applied Mechanics, Indian Institute of Technology Madras, Chennai, India

(Received 26 April 2012; accepted 20 July 2012; published online 30 August 2012)

A study is carried out to compare the non-linear behaviour of 1-3 piezocomposites with different volume fractions and bulk piezoceramics. Experiments are conducted to measure the electrical displacement and strain on piezocomposites and ceramics under high cyclic electrical loading. A thermodynamically consistent framework, combining the phenomenological and micromechanical models, is developed to predict the coupled behavior. Volume fractions of three distinct uni-axial variants (instead of six variants) are used as internal variables to describe the microscopic state of the material. In this model, the grain boundary effects are taken into account by introducing the back fields (electric field and stress) as non-linear kinematic hardening functions. In order to calculate the effective properties (elastic, piezoelectric, and dielectric constants) of piezocomposites for different volume fractions, an analytical model based on equivalent layered approach is proposed. The predicted effective properties are incorporated in the proposed model, and the classical hysteresis (electrical displacement versus electric field) as well as butterfly curves (strain versus electric field) is simulated. Comparison between the experiments and the simulations shows that this model can reproduce the characteristics of non-linear coupled response. It is observed that the variation in fiber volume fraction has a significant influence on the response of the 1-3 piezocomposites. © 2012 American Institute of Physics. [<http://dx.doi.org/10.1063/1.4748057>]

I. INTRODUCTION

Piezoelectric materials have a unique electromechanical coupling behavior that serves as a key aspect to smart material applications. Under the action of low electric fields or mechanical stress, the behavior of piezoelectric materials is almost linear but exhibits strong nonlinear response under high electric fields or mechanical stress; see the review articles.¹⁻³ Several experiments have been conducted and reported in the literature to understand the nonlinear behavior of piezoelectric materials.⁴⁻⁸ Constitutive modeling of piezoelectrics can be classified as macroscopic (phenomenological) and microscopic (sub grain) models. Phenomenological models are generally derived based on internal variables at any given time and the evolution of these internal variables is determined by the kinetic equations.⁹⁻¹² Micromechanical models are based on the internal microstructure and the domain switching mechanisms. Since the origin of the model includes more physical insight into the material, the model can predict the microstructural variations than phenomenological models from the modeling point of view.¹³⁻¹⁷

Though bulk piezoelectric materials are widely used in sensors and actuators, the brittle characteristics of lead zirconate titanate (PZT) ceramics can cause premature failure that limits their applications.¹⁸ A variety of piezocomposite materials can be made by combining piezoceramic elements with a passive polymer (epoxy) or active polymer.¹⁹ One popular piezocomposite is 1-3 composite, which contains piezoelectric rods (one dimension) embedded in a

polymer matrix (three dimension) and aligned along the thickness direction. Nowadays, bulk piezoelectric materials are replaced with 1-3 type piezocomposites in bio-medical transducers, underwater applications, and micropositioning systems wherein the materials are subjected to high loading conditions.²⁰ Since, the matrix materials are viscoelastic in nature, the influence of matrix in overall electro-mechanical response of piezocomposites is reported.²¹⁻²³

Literature review reveals that 1-3 type composites are good alternative for bulk PZT ceramics and it is necessary to understand the electro-mechanical behaviour of different fiber volume fractions. Hence, the objective of this work is to perform experiments and develop a theoretical framework based on the combination of micro-macro constitutive approach under high electric field. Subsequently, the overall performance of piezocomposites with different fiber volume fractions will be compared with the bulk piezoelectric materials (100% fiber volume). This comparative study helps in a better design of devices and increases its effective use in various applications. The outline of the paper is as follows: Sec. II describes the experimental setup and procedure. The experimental and theoretical prediction of effective properties of piezocomposites is discussed in Sec. III. The proposed non-linear model formulation for 1-3 type piezocomposite is elaborated in Sec. IV. Finally in Sec. V, the interpretation of experimental results and comparison with the theoretical results are reported.

II. EXPERIMENTAL DESCRIPTION

Experiments are conducted to measure the electrical displacement and the longitudinal strain of piezoelectric

^{a)}Electronic address: dhanujayen@gmail.com.

^{b)}Electronic address: aarajan@iitm.ac.in.

composites with different fiber volume fractions subjected to ac electric field along the fiber direction (poling direction). The bulk piezoceramic disc specimens (100 vol. % PZT5A1) of 10 mm diameter and 1 mm thickness are provided by Ceramtec. The chemical composition of PZT5A1 samples is lead zirconate titanate solid solutions. Similar thin disc samples of 1-3 piezocomposites with 80 vol. % [800 μm fiber diameter], 65 vol. % [250 μm fiber diameter], and 35 vol. % [105 μm fiber diameter] PZT5A1 fibers embedded into the epoxy matrix are supplied by Smart Materials Corporation. The schematic representation of the experimental set up to measure electrical displacement and strain is shown in Figure 1. Function generator (Tektronix AFG3022B) is used to generate required triangular wave form as an input signal to the amplifier. The generated signal is amplified to ± 2.5 kV using high voltage amplifier (TREK PD05034) and is supplied to the test specimen. The electrical displacement/polarization is measured using a modified Sawyer-Tower circuit.²⁴ The longitudinal displacement is measured using laser-interferometer (SIOS LSV-2500). All data are recorded with DAQ card (NI 9215) using LabVIEW.

III. PREDICTION OF EFFECTIVE PROPERTIES FOR 1-3 PIEZOCOMPOSITES

The material properties along the poling direction are necessary to develop a material model or design the material for sensing or actuation applications. Hence, an attempt has been made to measure the three material constants along the poling direction for bulk PZT and 1-3 piezocomposites of different fiber volume fraction using weak-field (<0.01 KV/mm) technique based on IEEE standards.²⁵ An analytical model is also proposed based on equivalent layered approach where the second phase layer thickness is proportional to the fiber volume fraction (Figure 2) to predict the effective properties of composites. The assumptions are employed based on the following fundamental concepts: (1) the overall homogenized stress equilibrium condition in the transverse directions (axes-1 and 2), (2) rule of mixtures in the longitudinal direction for stresses (axis-3), and (3) the homogenized displacement conditions for the longitudinal case in the theoretical calculations.^{26,27} Thus, the effective

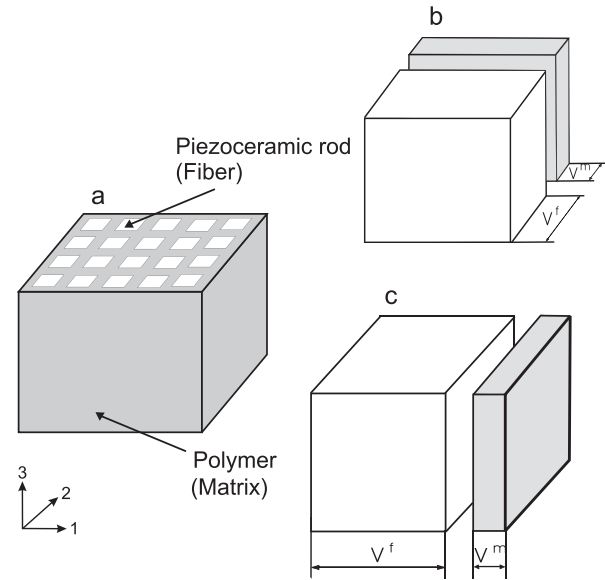


FIG. 2. Representation of a 1-3 piezoelectric composite as equivalent layered composite with proportional fiber and matrix volume fractions.

electro-mechanical coefficients of the composite are derived as

$$\begin{aligned} S_{33}^c &= v^f [2A_1 (S_{13}^f - S_{13}^m)] + v^f S_{33}^f + v^m S_{33}^m \\ d_{33}^c &= v^f [2A_1 (d_{31}^f - d_{31}^m)] + v^f d_{33}^f + v^m d_{33}^m \\ \kappa_{33}^c &= v^f [2A_2 (d_{31}^f - d_{31}^m)] + v^f \kappa_{33}^f + v^m \kappa_{33}^m, \end{aligned} \quad (1)$$

where v^f , v^m , S , d , and κ denote volume fraction of fiber, matrix, stiffness, piezoelectric constant, and dielectric permittivity, respectively. A_1 and A_2 are the functions of stiffness constants and volume fractions.

The input data for this model are stiffness, permittivity, and piezoelectric constants of fiber (bulk PZT) and matrix (epoxy); refer Table I. Figure 3 shows the variation of effective stiffness constant (S_{33}), dielectric permittivity (κ_{33}), and piezoelectric charge coefficient (d_{33}) using the proposed layered approach. The effective dielectric permittivity (κ_{33}) shows a linear variation with respect to fiber volume fraction. However, effective stiffness constant (S_{33}) and piezoelectric charge coefficient (d_{33}) show a non-linear variation at high (above 80%) fiber volume fraction due to the lateral clamping of the ceramic rods by the polymer matrix. To validate the model, the predicted results are compared with the measured data for the fiber volume fractions under study. The comparison shows a good agreement with deviation of around 5%–10%. Such deviations may be attributed to grain

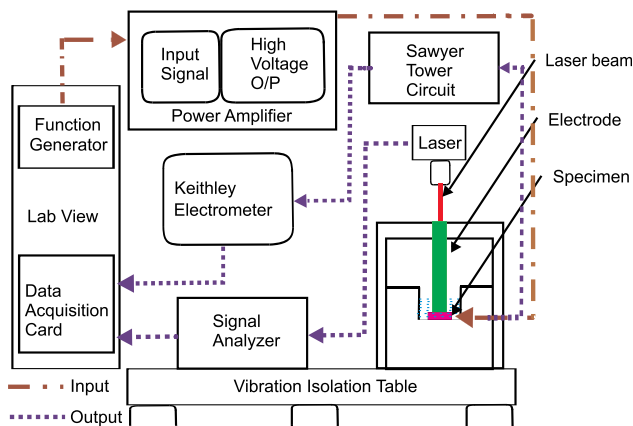


FIG. 1. Schematic diagram of experimental set up.

TABLE I. Material parameters of fiber and matrix (source: www.smart-material.com).

Material	S_{33} (GPa)	S_{13} (GPa)	κ_{33} (nF/m)	d_{33} (pC/N)	d_{31} (pC/N)
PZT5A1	116.8	87.1	16.4	440	-185
Epoxy	3.9	1.67	0.04	0	0

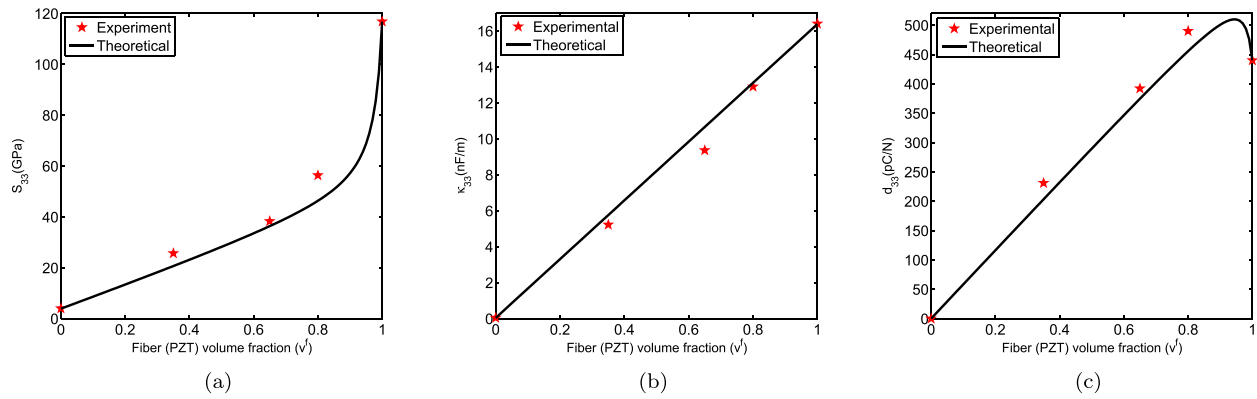


FIG. 3. Theoretical and experimental results showing the variation of constants with fiber volume fraction (stiffness (S_{33}), dielectric permittivity (κ_{33}), and piezoelectric charge coefficient (d_{33})).

boundary effects and distribution pattern of fiber, which is not considered in this model. Hence, this model can be used to predict the effective properties for further development in optimizing the piezocomposites.

IV. THEORETICAL FORMULATION

Given the tetragonal microstructure of polycrystalline piezoceramics, in the present work, a unit cell can orient in six different directions with respect to the crystallographic axes as shown in Figure 4 and each of them is referred as a variant or a domain. In a schematic representation, the six orientations can be grouped as in-plane (X, X', Z , and Z') and out-of-plane (Y and Y') variants. When the applied load exceeds a certain limit on piezoceramics, the domain will reorient in a way, the spontaneous polarization aligns according to the applied loading direction. This reorientation/change in domain is referred to as domain switching, which is irrecoverable in nature. Hence, the combination of reversible and irreversible response exhibits a hysteretic behaviour in piezoelectric materials that can be represented as

$$D = d : \sigma + \kappa \cdot E + P^I; \quad \epsilon = C : \sigma + d^T \cdot E + \epsilon^I, \quad (2)$$

where $D, E, \epsilon, \sigma, d, \kappa, C, P^I$, and ϵ^I denote dielectric displacement, electric field, mechanical strain, stress, piezo-electric coupling coefficient, dielectric permittivity, compliance constants, irreversible polarization, and strain, respectively. A thermodynamically consistent uni-axial model²⁸ is extended to study the non-linear behaviour of piezocomposites with

different volume fractions. Since experiments are conducted along the poling direction (i.e., Y and Y'), we reduce six possible tetragonal domain structures into three variants as two out-of-plane variants (Y and Y') and one in-plane variant (i.e., X, X', Z , and Z'). The volume fractions of out-of-plane and in-plane variants are represented as ξ^1, ξ^2 , and ξ^3 ; refer Figure 4. These three volume fractions are considered as internal variables representing the microscopic state of the piezoelectric polycrystal for this model. Hence, the significance of this model strongly depends on the choice of chosen internal variables, which combines both phenomenological and micro-mechanical aspects.

The remnant (irreversible) polarization and strain can be rewritten in terms of volume fractions as

$$\dot{P}^I = \sum_n \dot{P}^{(n)} \xi^{(n)}; \quad \dot{\epsilon}^I = \sum_n \dot{\epsilon}^{(n)} \xi^{(n)}; \quad n = 1, 2, 3, \quad (3)$$

satisfying the consistent conditions ($\xi^{(n)} \geq 0$; $\sum_n \xi^{(n)} = 1$; $\sum_n \dot{\xi}^{(n)} = 0$) at any instant. Since, the loading condition is “quasi-static,” a superscripted dot (\dot{x}) over a variable can be replaced by an incremental quantity Δ that renders

$$\Delta P^I = \sum_n N^{(n)} \Delta \xi^{(n)}; \quad \Delta \epsilon^I = \sum_n H^{(n)} \Delta \xi^{(n)}; \quad n = 1, 2, 3, \quad (4)$$

where $N^{(n)} = \dot{P}^{(n)}$ and $H^{(n)} = \dot{\epsilon}^{(n)}$. Using the laws of thermodynamics and appropriate initial as well as equilibrium conditions, the dissipation inequality of piezoelectric materials can be written as

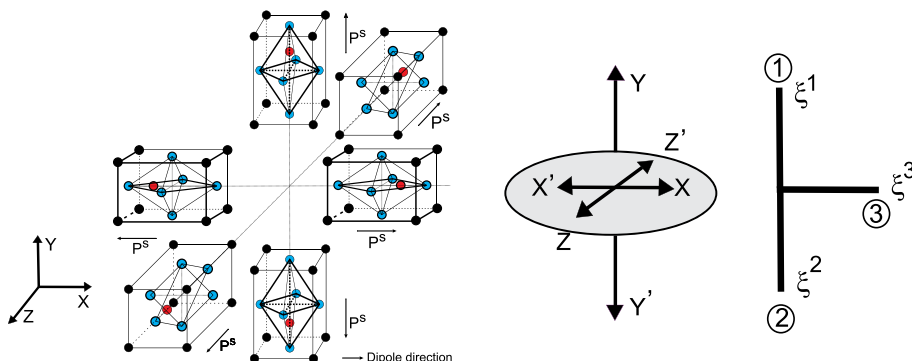


FIG. 4. Six different variants present in a tetragonal crystal structure, schematic representation of in-plane (X, X', Z , and Z') and out-of-plane (Y and Y') variants in a piezoceramic microstructure.

$$\sum_n \underbrace{[E\Delta N^{(m,n)} + \sigma\Delta H^{(m,n)} - \rho g_{\xi^{(m,n)}}]}_{D^{(m,n)}} \Delta \xi^{(n)} \geq 0$$

$$\Rightarrow \sum_n D^{(m,n)} \Delta \xi^{(n)} \geq 0; \quad m, n = 1, 2, 3 \text{ \& } m \neq n, \quad (5)$$

where $D^{(m,n)}$ denotes the driving force required for the domains to switch (n —new possible domain variants; m —present domain variant). To be specific, the driving forces for the transformation systems [(3,1), (3,2), and (2,1)] can be simplified as

$$D^{(m,n)} = \frac{N^{(n)}}{\Delta H} E + \sigma - \beta^E - \beta^\sigma; \quad m = 3, n = 1, \quad (6)$$

$$D^{(m,n)} = \frac{N^{(n)}}{\Delta H} E + \sigma + \beta^E - \beta^\sigma; \quad m = 3, n = 2, \quad (7)$$

$$D^{(m,n)} = 2E \frac{N^{(n)}}{\Delta H} - 2\beta^E; \quad m = 2, n = 1, \quad (8)$$

where $N^{(n)}$ and ΔH are changes in polarization and strain during the transformation process, respectively; E and σ are the applied electric field and stress, respectively; β^σ and β^E are denoted as back stress and electrical fields, respectively, which depend on the remnant strain and polarization that gets altered during the switching process. Therefore, the change in volume fraction of variants during domain switching can be related to the change in back fields as

$$\Delta \beta^\sigma = h_1 \Delta \epsilon^I = h_1 \sum_n H^{(n)} \Delta \xi^{(n)};$$

$$\Delta \beta^E = h_2 \Delta P^I = h_2 \sum_n N^{(n)} \Delta \xi^{(n)}; \quad n = 1, 2, 3. \quad (9)$$

h_1 and h_2 are hardening parameters as follows:

$$h_1(\epsilon^I) = \frac{2\beta_{max}^\sigma}{H_{max}\pi \left[1 - \left(\frac{2\epsilon^I}{H} - 1 \right)^2 \right]^{\frac{1}{n}}};$$

$$h_2(P^I) = \frac{2\beta_{max}^E}{N_{max}\pi \left[1 - \left(\left(\frac{P^I}{N} + 1 \right) \frac{1}{2} - 1 \right)^2 \right]^{\frac{1}{n}}}, \quad (10)$$

where β_{max}^σ , β_{max}^E , H_{max} , N_{max} , H , and N are maximum back field due to stress, electrical field, saturation strain, saturation polarization, remnant strain, and polarization respectively. In this work, the hardening parameters are introduced as a

function of remnant polarization and strain. Henceforth, the back electric field and stress represent the boundary effects in the polycrystalline structure. From the above discussions, the evolution equation of each variant for all possible transformation systems is derived using backward Euler method as follows:

$$\Delta \xi^{(n)} = \frac{D^{(m,n)} - k_1}{h_1 \Delta H + h_2 N^{(1)}}; \quad m, n = 3, 1 \text{ \& } m \neq n, \quad (11)$$

$$\Delta \xi^{(n)} = \frac{D^{(m,n)} - k_2}{h_1 \Delta H + h_2 N^{(1)}}; \quad m, n = 3, 2 \text{ \& } m \neq n, \quad (12)$$

$$\Delta \xi^{(n)} = \frac{D^{(m,n)} - k_3}{4h_2 N^{(1)}}; \quad m, n = 2, 1 \text{ \& } m \neq n, \quad (13)$$

where k_1 , k_2 , and k_3 are the critical values associated with the 90° and 180° domain switching. The above evolution equations are obtained based on the assumption that only one transformation is activated at a given instant. However, in piezoceramics there is a possibility for all the existing variants to simultaneously involve in the switching process. The evolution of more than two distinct variants for the given load increments is derived as

$$\Delta \xi^{(n)} = \frac{1}{2} \left[\frac{\Delta \beta^E}{h_2 N^{(n)}} + \frac{\Delta \beta^\sigma}{h_1 \Delta H} \right]; \quad n = 1, 2, \quad (14)$$

$$\Delta \xi^{(3)} = -\sum_n \Delta \xi^{(n)}; \quad n = 1, 2, \quad (15)$$

where $\Delta \beta^E$ and $\Delta \beta^\sigma$ refer to the back fields for simultaneous evolution process. By considering the possibility of simultaneous evolutions, the change in volume fractions is updated during the switching process. The macroscopic response of the piezoceramics is determined as the sum of reversible (R) and remnant (I) parts of polarization and strain for a particular loading condition:

$$P = \sum \left(P^{R(n)} + P^{I(n)} \right) \xi^{(n)} = \sum_n [d\sigma + \kappa E + N^{(n)}] \xi^{(n)};$$

$$n = 1, 2, 3, \quad (16)$$

$$\epsilon = \sum \left(\epsilon^{R(n)} + \epsilon^{I(n)} \right) \xi^{(n)} = \sum_n [C\sigma + dE + H^{(n)}] \xi^{(n)};$$

$$n = 1, 2, 3, \quad (17)$$

where C , d , and κ denote the compliance modulus, piezoelectric coefficient, and dielectric permittivity, respectively.

TABLE II. Material parameters used in model calculation.

v^f (%)	S_{33} (GPa)	κ_{33} (nF/m)	d_{33} (pC/N)	N (C/m ²)	H (%)	N_{max} (C/m ²)	H_{max} (%)	k_1 (GPa)	k_2 (GPa)	k_3 (GPa)	β_{max}^E (MN/C)	β_{max}^σ (GPa)
100	116.8	16.4	440	0.35	0.45	0.39	0.60	13	13	26	8	30
80	56.3	12.9	490	0.29	0.30	0.35	0.59	23	23	46	6	25
65	38.3	9.4	392	0.21	0.27	0.26	0.52	23	23	46	5	20
35	25.7	5.3	231	0.10	0.21	0.12	0.45	23	23	46	3	15

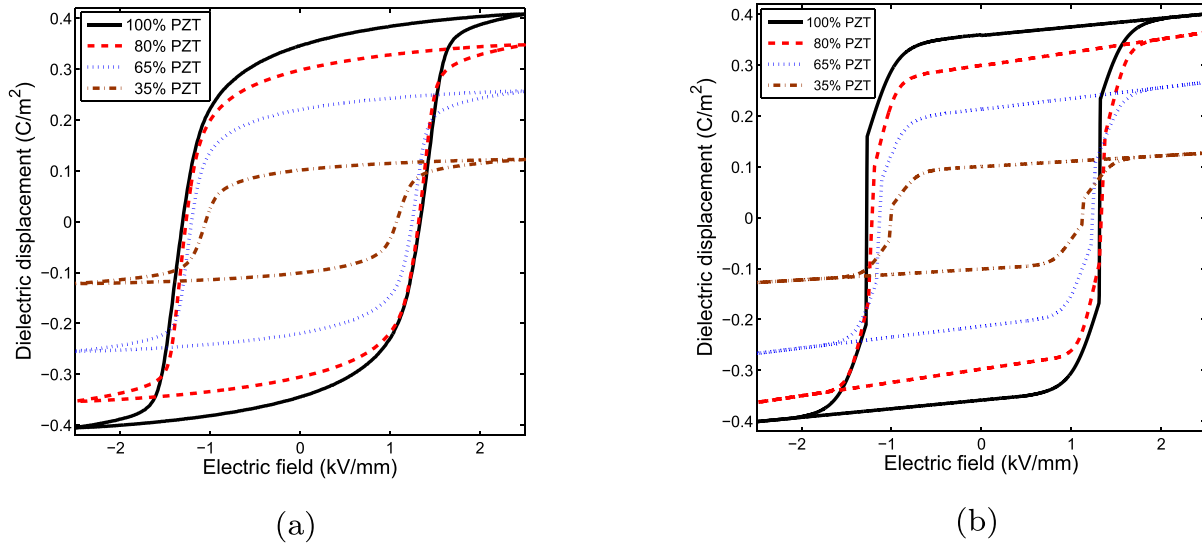


FIG. 5. Hysteresis loop [dielectric displacement vs. electric field]: (a) experimental, (b) theoretical.

V. RESULTS AND DISCUSSIONS

Experiments are conducted on piezocomposite specimens with 1, 0.8, 0.65, and 0.35 fiber volume fractions (v^f). To understand the behaviour of composite specimen in the non-linear regime, it is subjected to a tri-angular bipolar electric field with an amplitude beyond the coercive field. When the applied electric field reaches a coercive or critical electric field (E_c), domains start to switch in the direction of the applied electric field. Post the switch over of all the domains, the irreversible polarization and strain get saturated following which the response becomes linearly piezoelectric. The input parameters that are used in the model calculations are tabulated (Table II). The three effective parameters, namely, stiffness (S_{33}), dielectric permittivity (κ_{33}), and piezoelectric constant (d_{33}) are predicted based on the layered approach; refer Sec. III. The other parameters such as remnant polarization (N), remnant strain (H), saturation polarization (N_{max}), and saturation strain (H_{max}) are obtained from

the experimental data. The critical energy barrier (k_1, k_2, k_3) and maximum back fields ($\beta_{max}^E, \beta_{max}^\sigma$) are freely adjustable parameters to fit the experimental behavior.

Figures 5 and 6 show the measured and simulated dielectric hysteresis and butterfly loops of 1-3 piezocomposites for different volume fractions at room temperature. It is observed that fiber volume fraction has a significant effect on remnant polarization, saturation polarization, and coercive electric field. The decrease in fiber volume fraction shows the decrease in saturation polarization, remnant polarization, saturation strain, and remnant strain; refer Figure 7. The reason for the reduction in behaviour is obvious as the epoxy matrix is passive to the applied electrical field. Hence, it does not take part in piezo-electric coupling effects. The passivity also has an impact on reduction of coercive electric field with decrease in the fiber volume fraction. Since the number of dipoles reduces with decrease in fiber volume fraction, the resistance offered by the dipoles to switch decreases. The simplified model is capable of

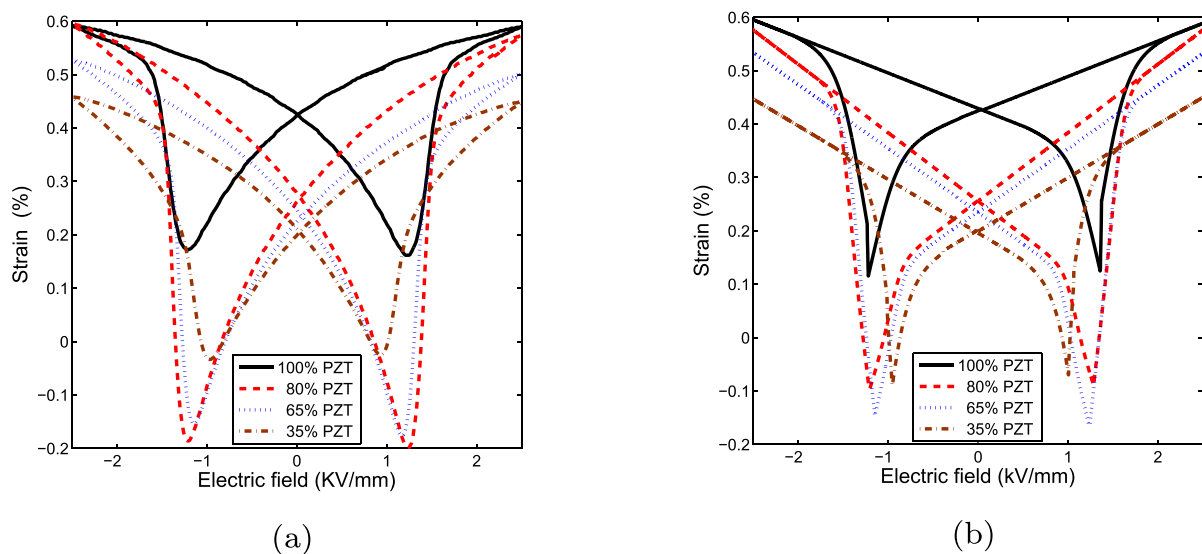


FIG. 6. Butterfly loop [strain vs. electric field]: (a) experimental, (b) theoretical.

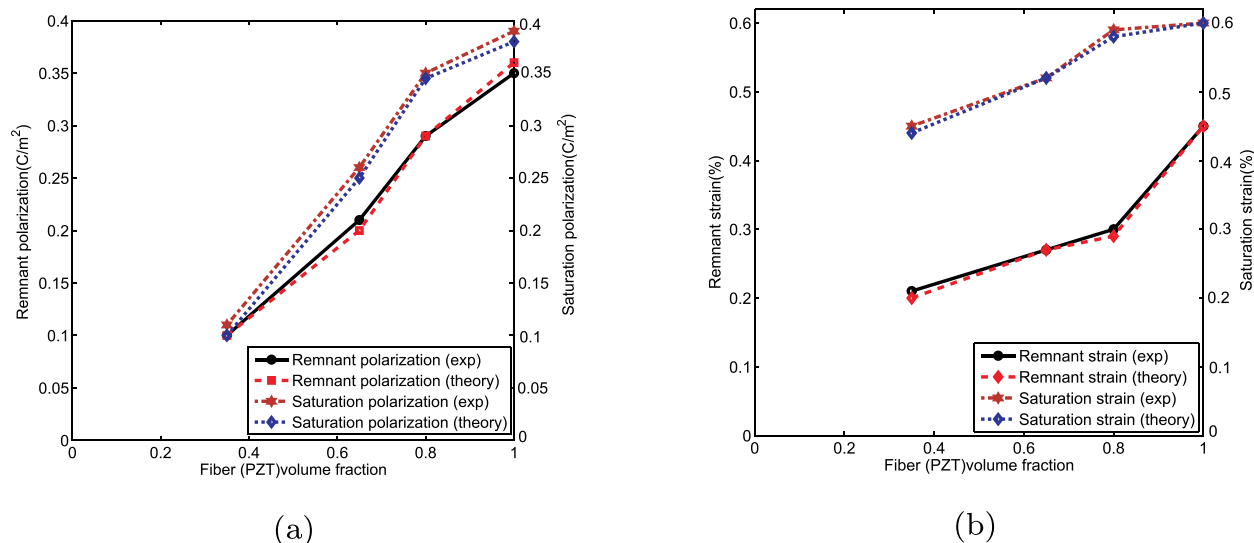


FIG. 7. Variations on output parameters of 1-3 piezocomposites.

TABLE III. Variations in output parameters of 1-3 piezocomposite compared with bulk PZT (100% fiber).

v^f (%)	Variations in remnant polarization (%)		Variations in remnant strain (%)		Variations in saturation polarization (%)		Variations in saturation strain (%)	
	Expt.	Model	Expt.	Model	Expt.	Model	Expt.	Model
80	17	19	33	35	10	09	02	03
65	40	44	40	40	33	34	13	13
35	71	72	53	55	72	73	25	26

predicting the nonlinear behaviour of 1-3 piezocomposites and is in good correlation with the experimental results. Hence, the developed model can be used to simulate the electro-mechanical response for any combinations of volume fractions.

The percentage variation on various output parameters from this study is tabulated in Table III for 35%, 65%, and 80% fiber volume fraction compared with bulk PZT (100% fiber). This study will help in designing the devices with appropriate section of fiber volume fraction for piezocomposites instead of bulk piezo material by comparing the various parameters (for instance, in actuator applications it is important to obtain large mechanical strain. However, by increasing the matrix volume fraction, there will be a reduction in mechanical strain). Hence, from this study a suitable fiber and matrix volume fractions can be chosen for device design depending upon the requirements.

VI. SUMMARY

The experiments are conducted to study the non-linear characteristics of 1-3 piezocomposites with different fiber volume fractions. A simple analytical model is proposed for the evaluation of effective material properties of piezoelectric fiber composites using homogenization technique based on equivalent layered approach. The predicted effective material properties based on the proposed model are compared with the experimental values and are found to be in good

agreement. A thermodynamically consistent uni-axial model combining the effects of both phenomenological and micro-mechanical approaches is developed for non-linear behavioural studies. In this model, non-linear kinematic hardening parameter is incorporated which is capable of capturing the realistic behaviour of 1-3 piezocomposites. The theoretical prediction shows a good comparison with the measured experimental results. The experimental and theoretical prediction shows a strong dependence on behaviour of 1-3 piezocomposites with the variation of fiber volume fraction. This study gives an insight into the design of devices for certain bio-medical and underwater applications wherein 1-3 composite can be replaced with bulk piezoceramics.

ACKNOWLEDGMENTS

The authors would like to acknowledge the financial support by the Department of Science and Technology—Fast track scheme (SR/FTP/ETA-006/2009) and CSIR—Research scheme (22(0580)/12/EMR-II). The authors gratefully acknowledge fruitful technical discussions with Professor M. S. Sivakumar (IIT Madras, India) and Dr. K. Jayabal (TU Dortmund, Germany).

¹M. Kamlah, *Continuum Mech. Thermodyn.* **13**, 219 (2001).

²C. M. Landis, *Curr. Opin. Solid State Mater. Sci.* **8**, 59 (2004).

³J. E. Huber, *Curr. Opin. Solid State Mater. Sci.* **9**, 100 (2005).

⁴H. Cao and A. G. Evans, *J. Am. Ceram. Soc.* **76**, 890 (1993).

⁵C. S. Lynch, *Acta Mater.* **44**, 4137 (1996).

- ⁶M. H. Lente and J. A. Eiras, *J. Appl. Phys.* **92**, 2112 (2002).
- ⁷M. Davis, D. Damjanovic, and N. Setter, *J. Appl. Phys.* **100**, 084103 (2006).
- ⁸S. Zhukov, Y. A. Genenko, and H. V. Seggern, *J. Appl. Phys.* **108**, 014106 (2010).
- ⁹M. Kamlah and C. Tsakmakis, *Int. J. Solids Struct.* **36**, 669 (1999).
- ¹⁰R. M. McMeeking and C. M. Landis, *Int. J. Eng. Sci.* **40**, 1553 (2002).
- ¹¹M. Elhadrouz, T. B. Zineb, and E. Patoor, *J. Intell. Mater. Syst. Struct.* **16**, 221 (2005).
- ¹²J. Lou, *J. Appl. Phys.* **105**, 094112 (2009).
- ¹³W. Lu, D. N. Fang, C. Q. Li, and K. C. Hwang, *Acta Mater.* **47**, 2913 (1999).
- ¹⁴J. Li, *J. Appl. Phys.* **94**, 3326 (2003).
- ¹⁵J. E. Huber and N. A. Fleck, *Eur. J. Mech. A/Solids* **23**, 203 (2004).
- ¹⁶G. J. Weng, *J. Appl. Phys.* **106**, 074109 (2009).
- ¹⁷A. Arockiarajan, S. M. Sivakumar, and C. Sansour, *Smart Mater. Struct.* **19**, 015008 (2010).
- ¹⁸L. J. Nelson, *Mater. Sci. Technol.* **18**, 1245 (2002).
- ¹⁹R. E. Newnham, D. P. Skinner, and L. E. Cross, *Mater. Res. Bull.* **13**, 525 (1978).
- ²⁰V. Y. Topolov and C. R. Bowen, *Electromechanical Properties in Composites Based on Ferroelectrics* (Springer, London, 2009).
- ²¹J. Aboudi, *Smart Mater. Struct.* **14**, 715 (2005).
- ²²A. H. Muliana, *Acta Mater.* **58**, 3332 (2010).
- ²³Y. Shindo, F. Narita, and T. Watanabe, *Eur. J. Mech. A/Solids* **29**, 647 (2010).
- ²⁴D. Zhou, M. Kamlah, and D. Munz, *J. Am. Ceram. Soc.* **88**, 867 (2005).
- ²⁵IEEE Standard on Piezoelectricity, ANSI/IEEE Std. 176–1987 (1988).
- ²⁶R. Kar-Gupta and T. Venkatesh, *Acta Mater.* **55**, 1093 (2007).
- ²⁷M. Sakthivel and A. Arockiarajan, *Comput. Mater. Sci.* **48**, 759 (2010).
- ²⁸K. Jayabal, D. Srikrishna, T. S. Abhinandan, A. Arockiarajan, and S. M. Srinivasan, *Int. J. Eng. Sci.* **47**, 1014 (2009).